European Journal of Radiology 150 (2022) 110233

Contents lists available at ScienceDirect

European Journal of Radiology

journal homepage: www.elsevier.com/locate/ejrad

Left ventricular four-dimensional blood flow distribution, energetics, and vorticity in chronic myocardial infarction patients with/without left ventricular thrombus

Ahmet Demirkiran [a], Mariëlla E.C.J. Hassell [b], Pankaj Garg [c], Mohammed S.M. Elbaz [d,e], Ronak Delewi [f], John P. Greenwood [c], Jan J. Piek [f], Sven Plein [c], Rob J. van der Geest [e], Robin Nijveldt [a,b,*]

[a] Department of Cardiology, Amsterdam UMC, Vrije Universiteit Amsterdam, Amsterdam Cardiovascular Sciences, Amsterdam, the Netherlands
[b] Department of Cardiology, Radboud University Medical Center, Nijmegen, the Netherlands
[c] Multidisciplinary Cardiovascular Research Centre & Leeds Institute of Cardiovascular and Metabolic Medicine, University of Leeds, Leeds, United Kingdom
[d] Department of Radiology, Feinberg School of Medicine, Northwestern University, Chicago, IL, USA
[e] Department of Radiology, Division of Image Processing, Leiden University Medical Center, Leiden, the Netherlands
[f] Department of Cardiology, Amsterdam UMC, Universiteit van Amsterdam, Amsterdam, the Netherlands

ARTICLE INFO

Keywords:
4D flow cardiovascular magnetic resonance imaging
Myocardial infarction
Direct flow
Kinetic energy
Vorticity
Vortex ring

ABSTRACT

Background: Left ventricular thrombus (LVT) formation is a frequent and serious complication of myocardial infarction (MI). How global LV flow characteristics are related to this phenomenon is yet uncertain. In this study, we investigated LV flow differences using 4D flow cardiovascular magnetic resonance (CMR) between chronic MI patients with LVT [MI-LVT(+)] and without LVT [MI-LVT(-)], and healthy controls.

Methods: In this prospective cohort study, the 4D flow CMR data were acquired in 19 chronic MI patients (MI-LVT (+), n = 9 and MI-LVT(-), n = 10) and 9 age-matched controls. All included subjects were in sinus rhythm. The following LV flow parameters were obtained: LV flow components (direct, retained, delayed, residual), mean and peak kinetic energy (KE) values (indexed to instantaneous LV volume), mean and peak vorticity values, and diastolic vortex ring properties (position, orientation, shape).

Results: The MI patients demonstrated a significantly larger amount of delayed and residual flow, and a smaller amount of direct flow compared to controls ($p = 0.02$, $p = 0.03$, and $p < 0.001$, respectively). The MI-LVT(+) patients demonstrated numerically increased residual flow and reduced retained and direct flow in comparison to MI-LVT(-) patients. Systolic mean and peak LV blood flow KE values were significantly lower in MI patients compared to controls ($p = 0.04$, $p = 0.03$, respectively). Overall, the mean and peak LV vorticity values were significantly lower in MI patients compared to controls. The mean and peak systolic vorticity at the basal level were significantly higher in MI-LVT(+) than in MI-LVT(-) patients ($p < 0.01$, for both). The vortex ring core during E-wave in MI-LVT(+) group was located in a less tilted orientation to the LV compared to MI-LVT(-) group ($p < 0.01$).

Conclusions: Chronic MI patients with LVT express a different distribution of LV flow components, irregular vorticity vector fields, and altered diastolic vortex ring geometric properties as assessed by 4D flow CMR. Larger prospective studies are warranted to further evaluate the significance of these initial observations.

1. Introduction

The formation of a left ventricular thrombus (LVT) is a serious complication of myocardial infarction (MI), leading to an increased systemic embolism risk [1,2]. A recent *meta*-analysis of over 2,000 patients showed an overall LVT incidence after acute MI of 6.3%, rising to 12.2% in those with anterior MI and 19.2% in those with anterior MI and LV ejection fraction < 50% [3]. However, the pathogenesis, particularly

* Corresponding author at: Radboudumc – Dpt of Cardiology, Geert Grooteplein Zuid 10, 6525 GA Nijmegen, The Netherlands, Amsterdam University Medical Centers (location VUmc) – Dpt of Cardiology, De Boelelaan 1117, 1081 HV Amsterdam, The Netherlands.
E-mail addresses: robin@nijveldt.net, robin.nijveldt@radboudumc.nl (R. Nijveldt).

https://doi.org/10.1016/j.ejrad.2022.110233
Received 3 June 2021; Received in revised form 23 February 2022; Accepted 26 February 2022
Available online 3 March 2022

the role of individual LV flow characteristics, remains unknown.

Cardiovascular magnetic resonance (CMR) enables four-dimensional (4D) flow analysis, which provides a 3-dimensional (3D) and 3-directional flow analysis in the left ventricle [4]. Recently, 4D flow data-derived energetics in the left ventricle were investigated in a combination of acute and chronic MI patients, and it was demonstrated that MI patients with LVT demonstrated reduced wash-in of blood to the distal left ventricle during late diastole [5]. Importantly, as LV remodelling occurs, and the infarct size diminishes over time, the LV blood flow energy levels may differ in chronic settings. Therefore, a further understanding of LVT formation and LV blood flow energetics in chronic MI patients is needed.

Previous echocardiography studies reported an association between LVT formation after MI and abnormal flow profiles, including LV spatial flow pattern and vortex ring formation, using 2-dimensional color Doppler flow echocardiography imaging [6–8]. However, these findings could not be expanded due to the lack of a modality that is capable of complex LV flow evaluation in its complete dimensionality. With recent advances in 4D flow analysis by CMR, functional intra-cardiac LV blood flow components (e.g., direct, retained) can be characterized, and vorticity and 3D vortex ring formation during diastole can be described. A comprehensive 4D flow analysis using these techniques may provide insights into the complex pathophysiological nature of the LVT formation after MI.

This study aimed to characterize 4D flow data-derived LV flow changes in chronic MI patients with and without LVT, and in healthy controls. We hypothesized that chronic MI patients with LVT might have reduced LV blood flow energetics, increased stagnant LV blood flow components, altered flow vorticity fields, and diastolic vortex ring formation in comparison to chronic MI patients without LVT.

2. Methods

This study was conducted according to the World Medical Association 2013 updated principles of the 1964 Declaration of Helsinki. The collection and management of data were approved by the National Research Ethics Service in the United Kingdom and the institutional Medical Ethical Committee in Leiden, The Netherlands. Written informed consent was obtained from all individual participants included in the study.

2.1. Study population

In this prospective cohort study, 19 patients with chronic MI (>3 months) and 9 age-matched healthy controls were included. The chronic MI patients were enrolled at the Leeds Teaching Hospitals NHS Trust, United Kingdom and consisted of 2 groups: 9 patients with LVT formation [MI-LVT(+)] and 10 patients without LVT formation [MI-LVT(-)]. Thrombus formation in the LV apex was identified from routine clinical echocardiography and CMR examinations. Only the chronic MI patients who had evidence of myocardial scar on late gadolinium enhancement (LGE) by CMR examination were included. The control subjects were recruited in 2 centers (Leeds, United Kingdom, n = 5 and Leiden University Medical Center, Leiden, the Netherlands, n = 4) and had no history of cardiovascular disease and were not on any medication. All included subjects were in sinus rhythm. Exclusion criteria were history of coronary artery bypass grafting, non-ischemic cardiomyopathy, significant renal impairment (defined as eGFR < 30 ml/min/1.73 m^2), haemodynamic instability, and any contraindication to CMR imaging. Finally, patients with valvular diseases (mild to severe) were also excluded to avoid potential intra-cardiac flow interference.

2.2. CMR protocol and analysis

All CMR examinations were performed on identical 1.5 T systems at the two study sites (Ingenia, Philips, Best, The Netherlands) with 28-channel flexible cardiac receiver coils. The CMR protocol included conventional cine imaging, LGE imaging, and at the end a 4D flow acquisition. ECG-gated, balanced steady-state free precession sequence was performed for the acquisition of long-axis cine imaging including 4-chamber, 3-chamber, and 2-chamber views and short-axis cine imaging covering the complete volume of the left ventricle. Each cine image series was acquired during 1 breath-hold at mild expiration. LV volumes, mass, and ejection fraction were measured on a consecutive stack of short-axis cines. LGE images were acquired 10–15 min after administration of a gadolinium-based contrast agent (Dotarem, Guerbet; 0.2 mmol/kg), using a T1-weighed segmented inversion-recovery gradient-echo pulse sequence in short-axis orientation covering the complete LV. Infarct size was calculated on the short-axis LGE images using the full-width-at-half-maximum method [9] and expressed as a percentage of the entire LV mass. For the assessment of LV blood flow characteristics (kinetic energy, particle tracing, vorticity, and vortex ring structure), 3D phase-contrast imaging with 3-directional velocity encoding (4D flow CMR) was used. Global blood flow data were acquired within the left ventricle using an Echo-Planar Imaging accelerated, a free-breathing sequence with retrospective ECG-triggering. In any type of phase-contrast flow imaging by CMR, concomitant gradient fields (Maxwell fields) and non-linear gradient fields result in spatially varying background phase offsets. Correction factors for these fields can be directly derived from the gradient waveforms used for the data acquisition. Relevant correction schemes are implemented and compensated on CMR scanner as part of the standard phase-contrast CMR image reconstruction [10–12]. Typical acquisition parameters were: TE/TR 3.7 ms/11 ms, flip angle 10°, VENC 150 cm/s and voxel size 3.0x3.0x3.0 mm (30 phases per cardiac cycle).

2.3. LV blood flow components and kinetic energy analysis

LV blood flow component analysis was performed using previously presented and validated methods [13] to demonstrate the component-specific routes and quantify the proportions of these LV flow components. In brief, the LV cavity was semi-automatically segmented in all temporal phases of the short-axis cine stack followed by a rigid registration of the short-axis stack with the 4D flow acquisition using the Elastix image registration toolbox [14]. Subsequently, particles were defined in the LV cavity at the moment of ED and particle tracing was performed to generate pathlines for each particle, backwards in time and forwards in time until the preceding or subsequent ES, respectively. LV blood flow was classified in four functional flow components according to the particles' position at ES, and the volume of each component was quantified as a proportion of the total end-diastolic volume [13,15]. LV flow components are identified as detailed in Table 1. Furthermore, the defined four LV flow components are visually described and demonstrated according to time points in the analyzed heart beat (peak systole, early diastole, late diastole) in Fig. 1 and supplementary video 1.

Kinetic energy (KE) is a form of energy that is a product of both the

Table 1
Definition of 4-dimensional left ventricular blood flow components.

Component	Definition
Direct flow	Blood that enters the LV during diastole and exits the LV during systole during the analyzed cardiac cycle, component of both inflow and ejected flow.
Retained inflow	Blood that enters the LV during diastole but does not exit during systole during the analyzed cardiac cycle; component of inflow only.
Delayed ejection flow	Blood that already resides inside the LV and exits during systole during the analyzed cardiac cycle: component of ejected flow only.
Residual volume	Blood that resides within the LV for at least two cardiac cycles; neither a component of inflow nor ejected flow.

Abbreviations: *LV; left ventricle.*

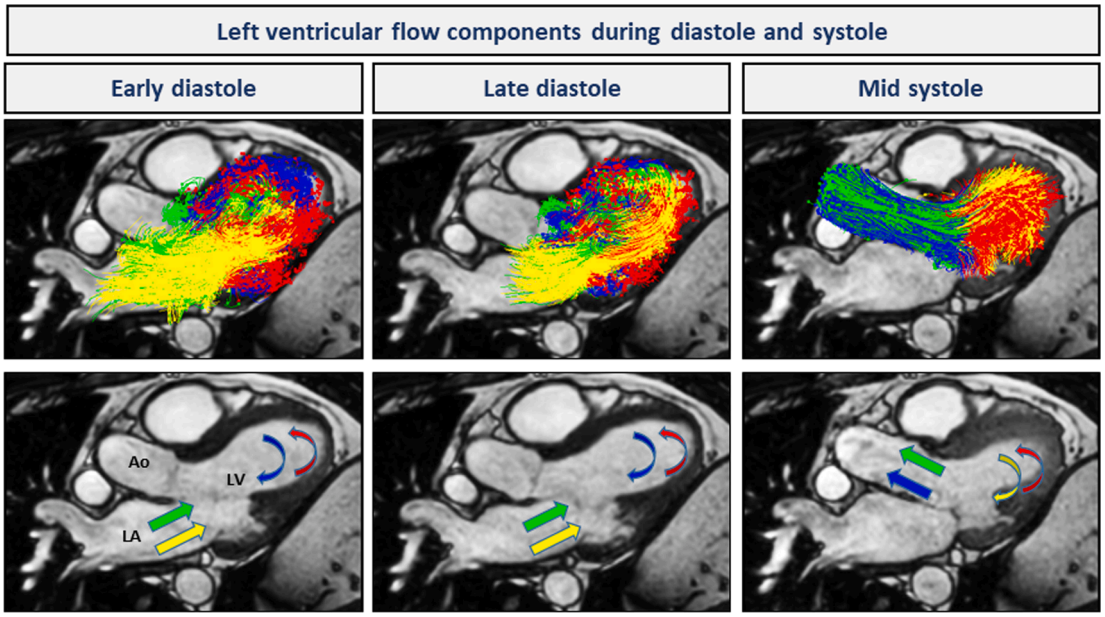

Fig. 1. Representation of left ventricle flow components during a cardiac cycle (early and late diastole, and mid-systole) on a 3-chamber cine view. Green particles (top) and arrow (bottom): direct flow; yellow particles and arrow; retained inflow; blue particles and arrow: delayed ejection flow; red particles and arrow: residual volume. Abbreviations. Ao: aorta, LV: left ventricle, LA: left atrium. (For interpretation of the references to color in this figure legend, the reader is referred to the web version of this article.)

motion and mass of moving objects/particles. As it is directly involved in the movement of blood, KE represents an important part of the total work of the heart [4,16]. In our study, blood flow KE within the LV was quantified for the region defined by the endocardial contours in the registered short-axis stack. For each voxel within the LV, KE was derived using the formula$KE = \frac{1}{2}mv^2$, with m the mass of a voxel, assuming a blood density of 1.06 g/mL, and v the velocity magnitude. Subsequently, the global KE in the left ventricle was computed by summation of KE over all voxels. LV mean and peak KE were quantified during the entire cardiac cycle, systole, diastole, E-wave, and A-wave. Fig. 2 visualizes left ventricular blood flow kinetic energy maps on a 2-chamber cine view at the peak E- and A-waves during diastole in relation with the corresponding time-curve of kinetic energy levels. E-wave corresponds to early passive blood flow from the left atrium to LV during early diastole, and A-wave reflects the active blood flow to LV which is generated by atrial contraction during late diastole. KE parameters were normalized to the instantaneous LV volume. In order to quantify the true KE, LVT was excluded from KE analysis in patients with LVT.

2.4. *Vortical flow patterns: Vorticity and vortex ring*

The blood flow inside the human heart is not a straight path and incorporates vortical flow patterns possessing rotational motion. Vortical flow patterns have different forms and shapes; they may constitute a small rotation around a voxel position or more prevalent as a dominant structure i.e., a vortex. Hence, there are different ways to characterize the vortical flow. 'Vorticity' is a mathematical measure of the degree of local rotation of blood around each voxel-position. It characterizes localized rotation of flow and can be measured at each voxel in the LV. This can be quantified voxel-wise using the 'vorticity' mapping which measures the amount of blood rotation around each voxel. On the other hand, a flow region (collection of voxels) rotating together around a common axis would form a 'vortex' structure. Being a structure, a vortex can have volume, position, and orientation. A vortex may have different shapes among which a vortex ring is the most stable; however, not every vortex is a vortex ring.

In the LV, during diastole, the interaction of the incoming blood inflow with the opening mitral valve leaflets results in the flow to roll-up into a vortex ring. If we are to take a cross-section through the LV

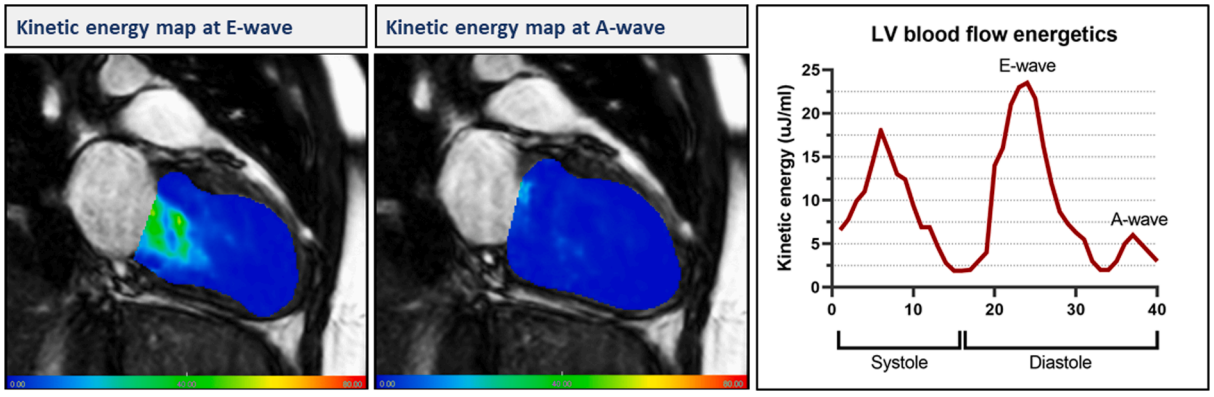

Fig. 2. Visualization of left ventricular blood flow kinetic energy at the peak E- and A-waves on a 2-chamber cine view and the corresponding time-curve of kinetic energy levels. The higher kinetic energy levels during E-wave compared to A-wave can be appreciated both on the kinetic energy maps and the time-curve.

diastolic 3D vortex ring in a 4-chamber view, a 3D vortex ring appears as two counter-rotating regions, one distal to the anterior MV leaflet and another distal to the posterior leaflet (Fig. 3). Vortex ring formation is particularly important because of its efficient flow organization and stability, making them ideal for transporting blood flow with minimum energy consumption. Elbaz et al. showed that diastolic vortex ring formation minimizes viscous energy loss by 2–4-fold compared to when it is not present [17]. As shown and discussed by Elbaz et al. [18]; vortex rings have two major roles: 1) rearranging the inflow into a compact organized structure that is more efficient to transport in bulk by maintaining flow momentum by preserving kinetic energy, 2) reorienting the organized 3D blood inflow towards the outflow tract for efficient blood ejection in the following systole; hence minimizing the mechanical energy (contraction) needed for blood ejection.

2.5. Vorticity analysis

The vorticity of the voxels was computed for every phase within the cardiac cycle using previously described methods [19,20]. The voxel-wise vorticity magnitude (1/s) was computed over the segmented LV volume using the endocardial contours in the registered short-axis stack. Subsequently, the average vorticity in the LV was quantified during the entire cardiac cycle, systole, diastole, E-wave, and A-wave. The formula that was used to calculate vorticity is shown in a supplementary file, "Appendix A".

2.6. Vortex ring analysis

The vortex ring cores appear in 3D as a closed torus-like shape distal to the mitral valve orifice. In our study, the diastolic 3D vortex ring was analyzed during both E and A waves employing vortex core analysis based on the 4D flow data using the method proposed by Elbaz et al. [18]. The position, orientation, and the shape of vortex ring in the left ventricle were analyzed as demonstrated in Fig. 4. The 3D vortex ring position in the left ventricle was characterized using a cylindrical cardiac coordinate system (circumferential (C), longitudinal (L), and radial (R)). The orientation of the vortex ring core relative to the LV long axis was quantified, and the ring shape was measured by the circularity index (CI), which is defined as the ratio between the vortex's short (D1) and long (D2) diameters.

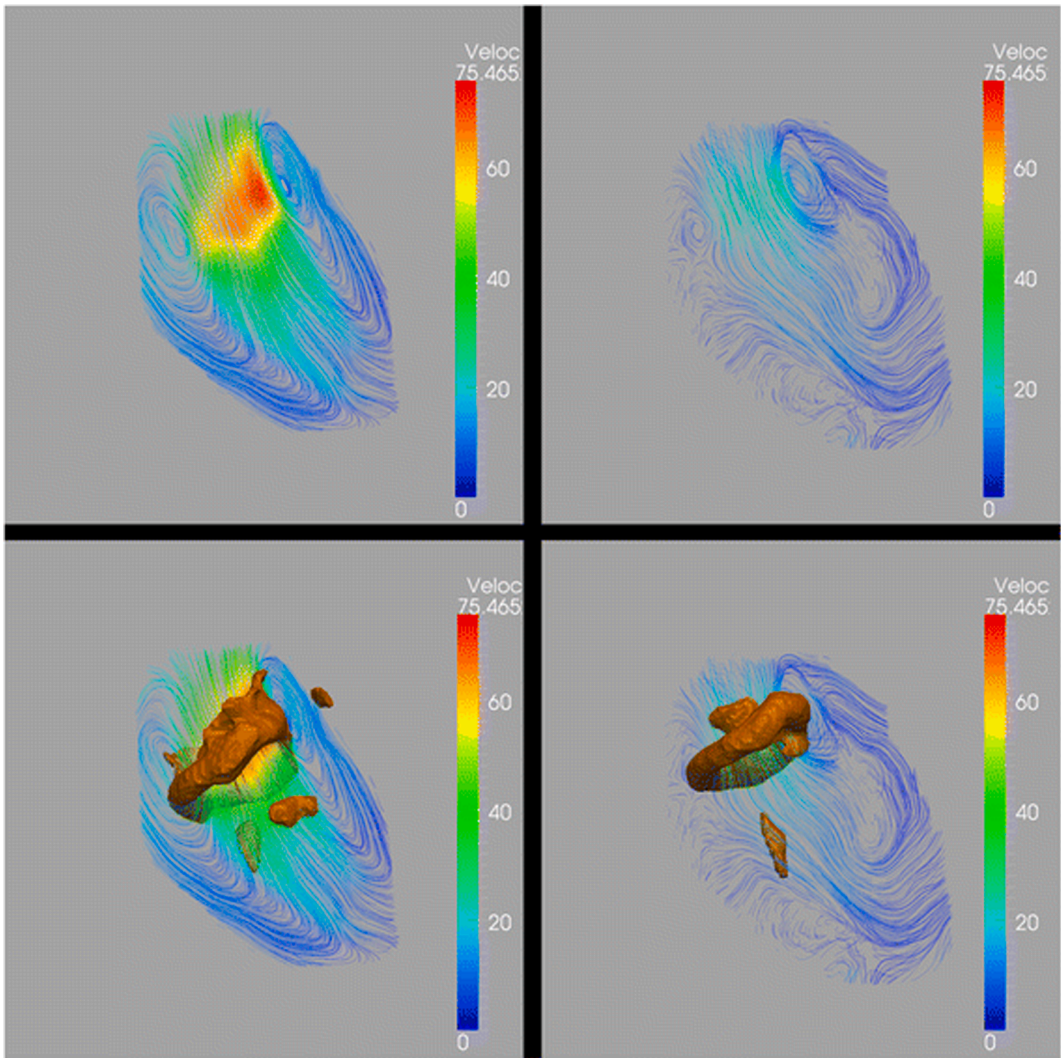

Fig. 3. Streamlines (instantaneous traces demonstrating the blood flow directions at specific time points) that are superimposed on vortex cores. Streamlines are visualized on a cross-sectional view of left ventricular flow during peak early filling (left-side) and peak late filling (right-side) showing pair of counter-rotating vortices. Streamlines are color coded (blue to red) based on velocity magnitude. Same frames are superimposed with 3D vortex ring cores showing the good overlap between the 3D vortex cores and the cores of corresponding 2D streamlines' counter-rotating vortices during both peak early and peak late filling. (*Reproduced with permission from* Elbaz et al. [18], *the Journal of Cardiovascular Magnetic Resonance 2014, 16:78*). (For interpretation of the references to color in this figure legend, the reader is referred to the web version of this article.)

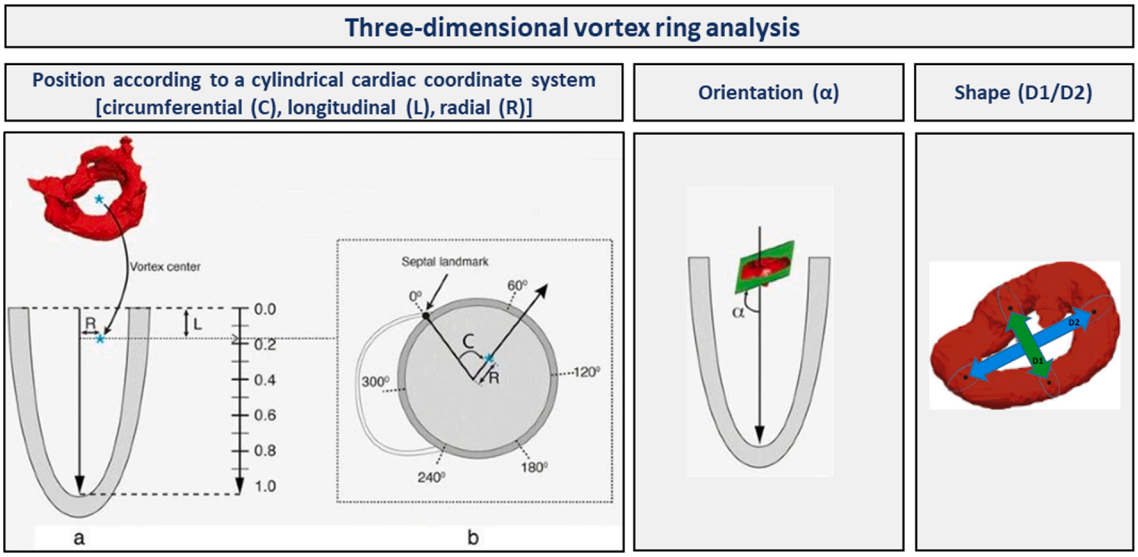

Fig. 4. The description and demonstration of the analysis of the 3-dimensional vortex ring. Definition of the local cardiac coordinate system (C, L, R) relative to the LV: The LV long-axis is defined as the line from the mid of the mitral valvular opening to the LV apex. The long-axis was calculated separately per filling phase (i.e. one for early filling and another for late filling). The center of the vortex ring was projected on this long-axis. The distance of the projected point to the mitral valve and to the vortex center defined the vortex's longitudinal (L) and radial (R) coordinates as illustrated in (a), respectively. Both L and R distances were normalized to the long-axis length and to the basal endocardial radius (measured on a reformatted short-axis slice), respectively to provide dimensionless parameters. Circumferential (C) Coordinate is defined as the angle between the septal landmark (the anterior attachment of the RV free wall with the LV) and the vortex center as illustrated in cross-sectional view (b). The vortex ring orientation (α) measured as an angle between the LV long-axis vortex and a fitting plane of the vortex ring, where an orientation of 90° means a vortex ring is perpendicular to the LV long-axis as shown in (c). The ring shape was measured by the circularity index (the ratio between the vortex's short (D1) and long (D2) diameters). (*Reproduced with permission from* Elbaz et al. [18]*, the Journal of Cardiovascular Magnetic Resonance 2014, 16:78*).

All CMR examination analyses were performed using dedicated research software (MASS version 2021-Exp, Leiden University Medical Center, Leiden, the Netherlands). All CMR contour tracings, including volume/function, LGE, and the 4D flow CMR were performed by M.H. and R.J.G. and controlled by EACVI level III certified CMR experts (P.G. and R.N.).

To allow for a straightforward and comprehensive understanding of the 4D flow data-derived intra-cardiac hemodynamic concepts that were exploited in the present study, the definitions of all concepts are briefly summarized in Table 2.

2.7. Statistical analysis

Continuous variables are presented as mean ± standard deviation or median with interquartile range, as appropriate. Comparisons between two groups were made with the independent-samples *T*-test for normally distributed data or Mann-Whitney *U* test for non-parametric data. Categorical variables are summarized by frequency (percentage), and relationships between categorical variables were tested with the $\chi 2$ test or Fisher-exact, if expected cell counts were low (<5). Association between continuous variables was quantified by Spearman's correlation. The two-sided significance level was set at 5%. As this was an explorative study, correction for multiple testing was not performed. Statistical analysis was performed using the Statistical Package for Social Sciences software (IBM SPSS statistics 26).

Table 2
Descriptions of 4-dimensional flow data-derived intra-cardiac hemodynamic concepts.

Concept	Description
Blood flow components	Specific blood flow routes/components through a compartment (e.g., left ventricle) during one cardiac cycle (e.g., direct flow, residual volume).
Kinetic energy	A form of energy that is a product of both the motion and mass of moving objects/particles.
Vorticity	A quantitative measure of the local rotation rate of blood flow particles around each voxel-position.
Vortex ring	Compact regions of circulating/swirling blood flow at the tips of the mitral valve leaflets during diastole.

3. Results

Baseline characteristics of the study population are summarized in Table 3. The mean age was comparable between MI patients and healthy controls and also between MI-LVT(-) and MI-LVT(+) groups. Whilst male frequency was n = 5 (56%) in controls, MI patients consisted of only male patients. With respect to medical history and smoking, no statistical difference was observed between MI-LVT(-) and MI-LVT(+) patients. All patients in the MI-LVT(-) group and 4 patients in the MI-LVT(+) group were treated with dual antiplatelet therapy. Furthermore, in the MI-LVT(+) group, 3 patients received a vitamin-K antagonist (VKA) and 1 patient a direct oral anticoagulant (DOAC) in combination with an antiplatelet.

All LV function, volume, and infarct findings are presented in Table 4. The MI patients demonstrated higher LV volumes (end-systolic and end-diastolic) and lower LV ejection fraction (LVEF) than controls ($p = 0.001$, $p = 0.001$, and $p < 0.001$, respectively). No significant differences were found for LVEF, LV volumes, and infarct size between the MI-LVT(-) and MI-LVT(+) groups.

3.1. LV blood flow components

The relative amount of the different LV blood flow components for all groups is illustrated in Fig. 5. The residual and direct flows constituted the largest components of LV flow within MI patients and controls (36 ± 11%, 38 ± 6%, respectively). The MI patients demonstrated significantly a larger amount of delayed flow, residual flow, and a smaller amount of direct flow in comparison to controls (23 ± 6% vs. 17 ± 6%, $p = 0.02$, 36 ± 11% vs. 27 ± 7%, $p = 0.03$, and 22 ± 7% vs. 38 ± 6%, $p < 0.001$, respectively). Although MI-LVT(+) patients

Table 3
Baseline characteristics.

	Controls (n = 9)	MI patients (n = 19)	P value	MI-LVT(-) (n = 10)	MI-LVT(+) (n = 9)	P value
Demographics						
Age (years)	57 ± 8	65 ± 14	0.15	62 ± 14	68 ± 15	0.33
Male (No. %)	5 (56%)	19 (100%)	<0.01	10 (100%)	9 (100%)	NA
BMI (kg/m^2)	23 ± 2	28 ± 4	0.01	30 ± 4	26 ± 3	0.03
Medical history (no, %)						
Hypertension	0	7 (37%)	0.06	3 (30%)	4 (44%)	0.11
Diabetes mellitus	0	3 (16%)	0.53	1 (10%)	2 (22%)	0.50
Hypercholesterolemia	0	6 (32%)	0.14	3 (30%)	3 (33%)	0.25
Smoking	0	9 (47%)	0.02	6 (60%)	3 (33%)	0.37
Culprit artery (no, %)						
Left anterior descending	NA	13 (72%)	NA	5 (50%)	8 (89%)	0.14
Left Circumflex	NA	1 (5%)	NA	1 (10%)	0	1.0
Right coronary artery	NA	4 (22%)	NA	4 (40%)	0	0.08
Antithrombotic medication						
DAPT (no, %)	0	14 (74%)	0.01	10 (100%)	4 (44%)	0.01
Antiplatelet + VKA (no, %)	0	3 (16%)	0.53	0	3 (33%)	0.08
Antiplatelet + DOAC (no, %)	0	1 (5%)	1.0	0	1 (11%)	0.47

Abbreviations: *MI, myocardial infarction; LVT, left ventricular thrombus; BMI, body mass index; DAPT, dual antiplatelet therapy; VKA, vitamin K antagonist; DOAC, direct oral anticoagulant.*

Table 4
LV volume, function, and infarct characteristics.

	Controls (n = 9)	MI patients (n = 19)	P value	MI-LVT(-) (n = 10)	MI-LVT (+) (n = 9)	P value
LVEF (%)	61 ± 6	45 ± 10	<0.001	49 ± 4	41 ± 13	0.11
LVEDV (ml)	135 ± 33	196 ± 44	0.001	186 ± 33	206 ± 54	0.34
LVEDVi (ml/m^2)	77 ± 15	99 ± 24	0.02	92 ± 12	106 ± 33	0.21
LVESV (ml)	53 ± 16	110 ± 45	0.001	95 ± 19	127 ± 60	0.12
LVESVi (ml/m^2)	30 ± 8	56 ± 27	0.01	47 ± 7	66 ± 37	0.12
LVEDM (g)	89 ± 31	112 ± 33	0.07	100 ± 15	127 ± 41	0.09
LVEDMi (g/m^2)	50 ± 13	57 ± 16	0.27	54 ± 9	65 ± 21	0.05
Infarct size (% of LV mass)	NA	17 ± 11	NA	15 ± 5	18 ± 15	0.67

Abbreviations: MI, myocardial infarction; LVT, left ventricular thrombus; LVEF, left ventricular ejection fraction; LVEDV, left ventricular end-diastolic volume; LVEDVi, left ventricular end-diastolic volume indexed; LVESV, left ventricular end-systolic volume; LVESVi, left ventricular end-systolic volume indexed; LVEDM, left ventricular end-diastolic mass; LVEDMi, left ventricular end-diastolic mass indexed; LV, left ventricle.

demonstrated increased residual flow and reduced retained and direct flow components in comparison to MI-LVT(-) patients, these were not statistically significant (40 ± 14% vs. 33 ± 7%, p = 0.15; 17 ± 5% vs. 20 ± 2%, p = 0.07; 21 ± 8% vs. 23 ± 5%, p = 0.39, respectively)..

3.2. LV blood flow kinetic energy

Table 5 provides a detailed assessment of the LV KE characteristics and the differences between the groups. The LV KE characteristics according to the basal, mid, and apical levels are reported in the supplemental file. Absolute mean and peak LV KE values were lower in MI patients compared to controls during the entire cardiac cycle as well as during systole and diastole, which indicates the altered energy levels in MI patients. The reduced mean and peak KE values in MI patients compared to controls were more apparent and significant during systole (10.27 ± 2.95 uJ/ml vs. 12.64 ± 2.31 uJ/ml p = 0.04 and 16.97 ± 5.19 uJ/ml vs. 21.34 ± 3.27 uJ/ml p = 0.03, respectively). With respect to the comparison of KE between the MI-LVT(-) and MI-LVT(+) patients, no significant differences were observed.

3.3. Vorticity and vortex ring

Table 6 summarizes the LV vorticity characteristics and the differences between the groups. The basal, mid, and apical-level LV vorticity characteristics are detailed in the supplemental file. The mean and peak LV vorticity values were significantly lower in MI patients compared to controls during the entire cardiac cycle as well as during systole and diastole (Fig. 6). In addition, there was an inverse and significant association between infarct size and all mean and peak vorticity values. Notably, mean and peak vorticity at the basal level were significantly lower in the MI-LVT(-) than MI-LVT(+) patients (254 ± 20 1/s vs. 300 ± 39 1/s and 308 ± 29 1/s vs. 361 ± 43 1/s, respectively, p < 0.01 for both) during systole. Fig. 7 illustrates LV flow vorticity levels on a healthy control and MI patients with and without LVT. LV vortex ring characteristics are detailed for all groups in Table 7. In the chronic MI group, the vortex ring core observed during E-wave was positioned significantly more anteriorly (lower circumferential value) in comparison to the control group (p = 0.01). During A-wave, the vortex ring core was positioned closer to the LV long-axis (lower radial value) in comparison to controls (p = 0.01). Furthermore, the vortex ring core during E-wave in MI-LVT(+) group was located closer to the mitral annulus (shorter longitudinal value) and in a less tilted orientation to the LV compared to the MI-LVT(-) group (p = 0.08, p < 0.01, respectively).

4. Discussion

This study provides a comprehensive insight into 4D LV flow changes in chronic MI patients with and without LVT, and healthy controls. Firstly, we found that MI patients have a more delayed LV blood flow component and reduced LV blood flow energetics than healthy controls, particularly during systole. Secondly, MI-LVT(+) patients reveal less direct and retained flow, but larger residual flow components in the LV in comparison to MI-LVT(-) patients. Thirdly, LV vorticity levels are significantly reduced in MI patients compared to controls and demonstrate a lower pattern in MI-LVT(-) patients compared to MI-LVT(+) patients, which is most apparent at the basal level during systole. Finally, MI-LVT(+) patients demonstrate a less tilted vortex ring core to the LV during E-wave compared to the MI-LVT(-) group.

The LVT formation is a frequent and serious adverse event of MI and can persist for long periods (>3 months). The pathophysiology of

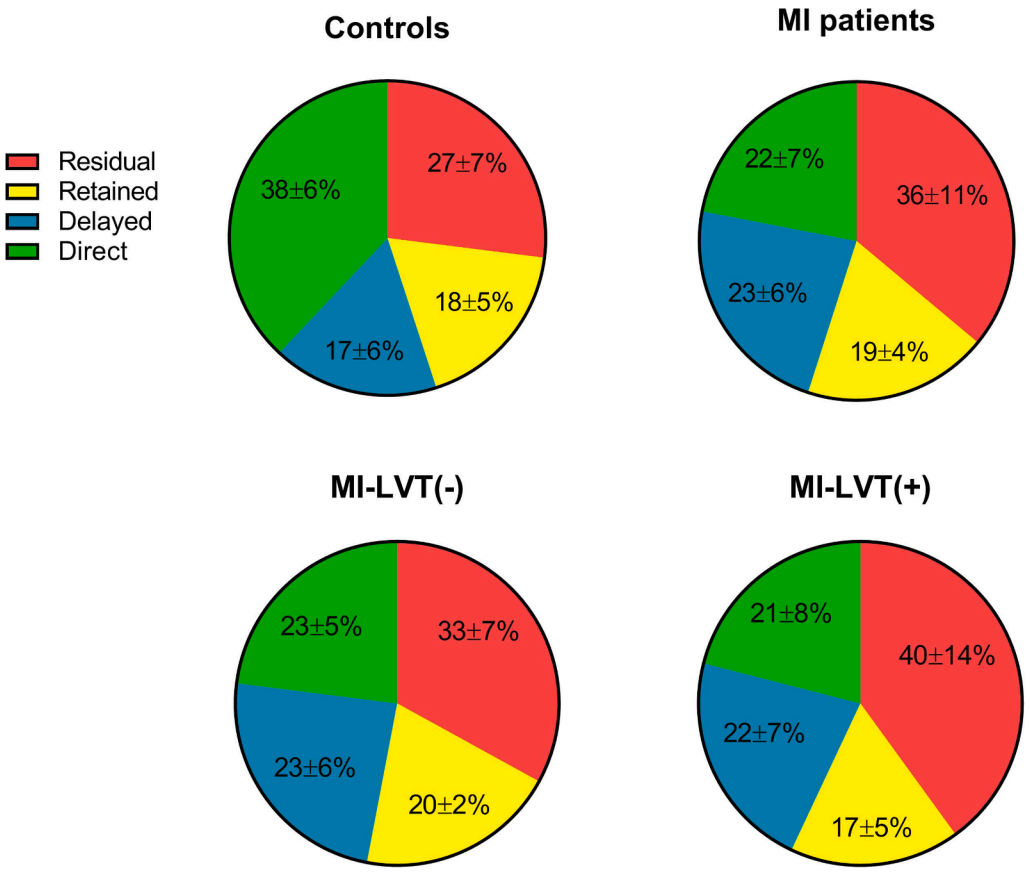

Fig. 5. Relative proportions of the end-diastolic left ventricular blood flow volume components in MI patients and its subgroups [MI-LVT(-), MI-LVT(+)], and healthy controls. Abbreviations: *MI, myocardial infarction; LVT, left ventricular thrombus.*

Table 5
LV blood flow kinetic energy characteristics.

	Controls (n = 9)	MI patients (n = 19)	P value	MI-LVT (-) (n = 10)	MI-LVT (+) (n = 9)	P value
LV blood flow KE (uJ/ml)						
KE mean (R-R interval)	10.61 ± 2.42	8.81 ± 2.40	0.07	8.33 ± 2.27	9.35 ± 2.56	0.37
KE peak (R-R interval)	28.41 ± 7.32	23.30 ± 8.20	0.12	23.37 ± 9.02	23.24 ± 7.72	0.97
KE mean (systole)	12.64 ± 2.31	10.27 ± 2.95	0.04	9.35 ± 1.92	11.29 ± 3.63	0.15
KE peak (systole)	21.34 ± 3.27	16.97 ± 5.19	0.03	15.21 ± 3.16	18.94 ± 6.41	0.12
KE mean (diastole)	9.52 ± 3.12	8.14 ± 2.79	0.24	7.85 ± 2.80	8.47 ± 2.90	0.64
KE peak (diastole)	28.41 ± 7.32	21.37 ± 9.07	0.05	22.20 ± 10.19	20.44 ± 8.15	0.68
KE peak (E-wave)	28.41 ± 7.32	20.90 ± 9.46	0.04	21.53 ± 10.75	21.53 ± 10.75	0.77
KE peak (A-wave)	13.30 ± 5.24	11.58 ± 5.22	0.38	10.79 ± 4.70	12.47 ± 5.91	0.49

Abbreviations: *MI, myocardial infarction; LVT, left ventricular thrombus; KE, kinetic energy,* min*, minimum;* max*, maximum.*

Table 6
LV vorticity characteristics.

	Controls (n = 9)	MI patients (n = 19)	P value	MI-LVT (-) (n = 10)	MI-LVT (+) (n = 9)	P value
LV vorticity (1/s)						
Vorticity mean (R-R interval)	285 ± 62	217 ± 32	0.01	207 ± 24	228 ± 39	0.18
Vorticity peak (R-R interval)	405 ± 68	318 ± 60	<0.01	311 ± 59	325 ± 64	0.62
Vorticity mean (systole)	302 ± 50	209 ± 30	<0.001	199 ± 21	221 ± 35	0.10
Vorticity peak (systole)	355 ± 44	264 ± 46	<0.001	255 ± 50	275 ± 42	0.36
Vorticity mean (diastole)	273 ± 73	223 ± 38	0.02	214 ± 28	234 ± 45	0.25
Vorticity peak (diastole)	386 ± 103	316 ± 61	0.03	311 ± 59	321 ± 67	0.74
Vorticity peak (E-wave)	384 ± 108	303 ± 62	0.01	296 ± 57	311 ± 70	0.61
Vorticity peak (A-wave)	307 ± 80	263 ± 55	0.10	256 ± 61	270 ± 51	0.57

Abbreviations: *MI, myocardial infarction; LVT, left ventricular thrombus.*

thrombus formation involves the three components of Virchow's triad: endothelial/endocardial damage or dysfunction, blood stasis, and hypercoagulability [21]. Yet, little is known about the role of individual LV flow characteristics on LVT formation. An elaborate evaluation of LV flow characteristics by 4D flow CMR may enhance understanding of the pathophysiology behind flow changes in chronic MI and the occurrence and persistence of LVT.

Organization of the LV blood flow patterns allows investigation of blood transportation efficiency. A higher percentage of direct flow is assumed to be associated with more efficient blood transport, thus more preserved KE, whereas resident flows (i.e., retained, residual) require more additional energy for ejection out of the LV [22]. Our findings

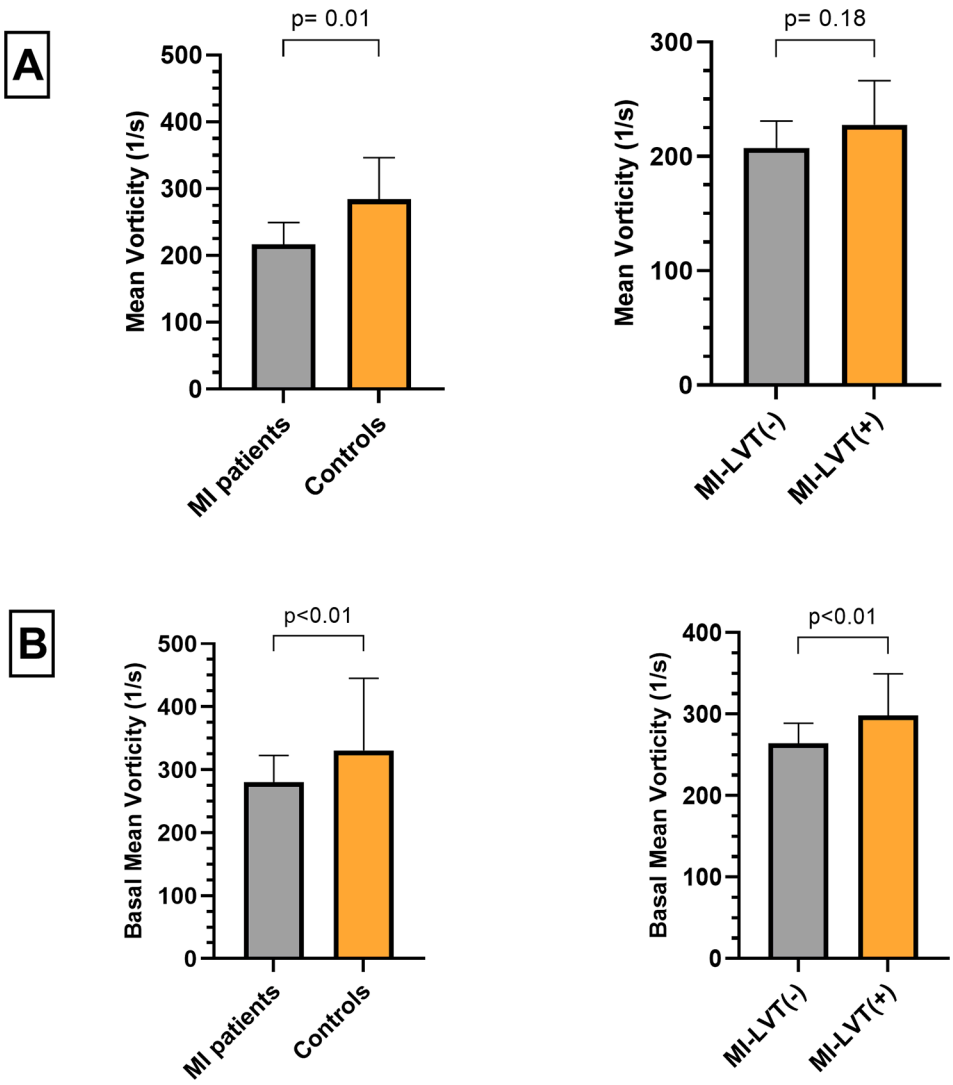

Fig. 6. Comparison of mean vorticity values in the entire LV during the whole cardiac cycle (A) and at the basal level during systole (B) between MI patients and healthy controls and between MI patients without thrombus, MI-LVT(-) and MI patients with thrombus, MI-LVT(+). Data are shown as mean and standard deviation. Abbreviations: *MI, myocardial infarction; LVT, left ventricular thrombus.*

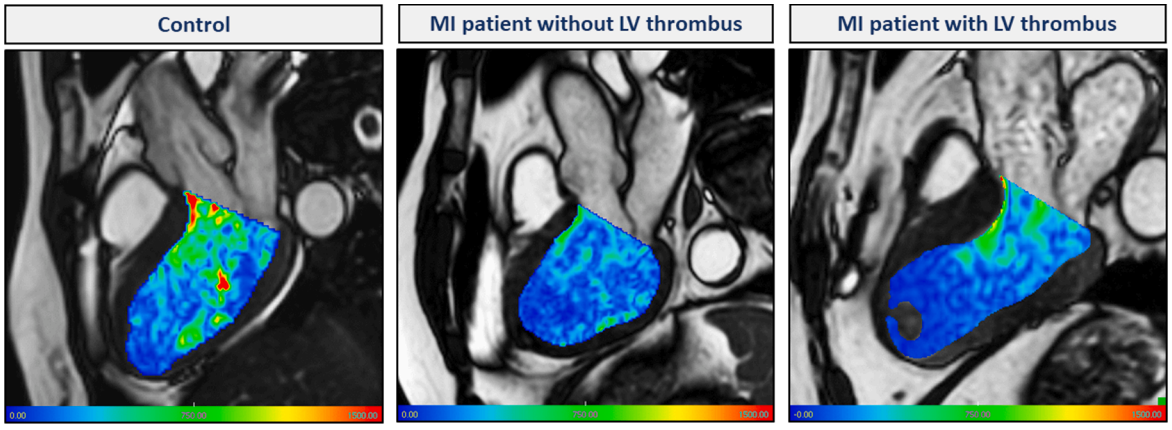

Fig. 7. Demonstration of LV vorticity on a 3-chamber view during systole in a healthy control, chronic MI patient without LV thrombus, and chronic MI patient with LV thrombus. In all subjects, the vorticity levels demonstrate an increasing pattern from apical towards basal level. In the healthy control, overall vorticity levels are higher than MI patients. The MI patient with LV thrombus presents higher vorticity levels at the basal level than the MI patient without LV thrombus, particularly in the vicinity of LV outflow tract. Abbreviations: *MI, myocardial infarction.*

Table 7
LV vortex ring characteristics.

	Controls (n = 9)	MI patients (n = 19)	P value	MI-LVT(-) (n = 10)	MI-LVT(+) (n = 9)	P value
During E-wave						
Circumferential (in degrees)	115 ± 44°	68 ± 45°	0.01	58 ± 36°	79 ± 53°	0.32
Longitudinal	0.20 ± 0.06	0.19 ± 0.05	0.66	0.21 ± 0.05	0.17 ± 0.03	0.08
Radial	0.23 ± 0.10	0.20 ± 0.10	0.54	0.21 ± 0.09	0.19 ± 0.12	0.75
Orientation (in degrees)	70° [62–77]	68° [56–81]	0.87	62° [53–67]	81° [71–97]	<0.01
Circularity index	0.76 ± 0.13	0.77 ± 0.10	0.78	0.76 ± 0.09	0.77 ± 0.11	0.77
During A-wave						
Circumferential (in degrees)	105 ± 39°	71 ± 45°	0.10	75 ± 40°	65 ± 55°	0.70
Longitudinal	0.79 ± 0.07	0.83 ± 0.04	0.10	0.81 ± 0.03	0.86 ± 0.42	0.10
Radial	0.19 ± 0.06	0.13 ± 0.04	0.01	0.13 ± 0.06	0.13 ± 0.03	0.99
Orientation (in degrees)	68° [64–70]	65° [56–74]	0.50	64° [57–68]	71° [56–91]	0.36
Circularity index	0.68 ± 0.09	0.66 ± 0.11	0.59	0.61 ± 0.05	0.72 ± 0.14	0.05

Abbreviations: *MI, myocardial infarction; LVT, left ventricular thrombus*.

demonstrate that MI patients had a larger proportion of delayed and residual LV flows but a smaller proportion of direct flow in comparison to controls. Recent research demonstrated similar derangements in LV flow in ischemic cardiomyopathy as well as dilated cardiomyopathy patients [23]. Moreover, it was demonstrated that LV blood flow distribution may be altered in heart failure patients with only mild LV remodelling [15,24]. In this present study, we described LV blood flow components for the first time in MI patients with LVT. We found that MI-LVT(+) patients had an altered LV flow distribution compared to MI-LVT(-) patients. The decreased direct and increased residual flows indicate the reduced efficiency of LV blood flow transportation in MI patients with LVT. The decreased retained flow component may be partly explained by the fact that the existence of LVT allows less space to reserve incoming flows in the LV. Nevertheless, these alterations were not significantly differed between the MI patients with and without LVT. This suggests that the persistence of LVT in the chronic stage after MI may not be fully explained by a derangement of LV flow components.

The KE work is directly related to the LV blood flow movement, thus it is of importance to explore its relevance to post-MI hemodynamics. In acute settings of myocardial injury, LV blood flow energetics likely alter, particularly as a result of hypercoagulability and myocardial dysfunction. The possible regression of a prothrombotic state and myocardial remodelling may influence the LV blood flow energetics over time. Garg et al. reported that LV blood flow KE values are reduced overall in MI patients, but they observed no significant LV blood flow KE changes between acute and chronic MI patients [5,25]. We observed that LV blood flow energetics even in the chronic phase of MI were still reduced compared to controls during the entire cardiac cycle. Of note, the reduction of LV blood flow energetics was more remarkable during systole. This may partly be explained by the increased pressure gradients within the LV during systole due to reduced mechanical force on the intra-cavity blood, as a consequence of regional hypocontractility. Moreover, we observed no significant differences regarding global blood flow KE values between MI-LVT(+) and MI-LVT(-) patients. One could speculate that the initial disturbance in LV blood flow energetics during the acute event of MI can be a more important factor than chronic stage energetics to explain the persistence of the LVT. Nevertheless, previous research revealed reduced wash-in of the LV blood flow KE in MI patients with LVT [5], thus more energy-focused studies in MI patients are needed to validate the current findings.

Vorticity refers to the local spinning of blood particles and numerous factors may affect the generation of vorticity including flow velocity gradients and flow directionality. The increase in vorticity can lead to favorable effects such as conservation of momentum by KE storage but also some adverse effects when the optimal flow direction is disturbed due to abnormal intra-cardiac structures [26]. Previously, this hemodynamic parameter was found to be associated with ventricular diastolic dysfunction in different clinical settings and reduced LV vorticity values were observed in patients with chronic obstructive pulmonary disease [19,20]. In this study, we investigate the vorticity in MI patients with LVT for the first time. The vorticity levels were significantly lower in MI patients than controls and there was a significant inverse relation between all vorticity parameters and infarct size. This could partly be explained by the enlarged LV volume (more space for the circulation of the LV blood) and the altered structure-flow interactions between the LV flow and wall motion abnormalities. Furthermore, we observed increased vorticity fields in MI patients with thrombus than without thrombus throughout the LV and these differences reached significance at the basal level during systole. As there was no significant differences for LV function and volumes between the MI patients with and without thrombus, the vorticity changes may be indeed attributed to the existence of thrombus. LVT formations are likely to interfere with the flow directions at any point that LVT interacts with the LV blood. The impact of LVT on velocity gradient and direction changes, thus vorticity differences may become more evident towards basal levels, as the blood flow becomes less stagnant (increased KE). These initial observations may provide insights into the emerging hemodynamics in the chronic phase after MI.

Early studies on vortex formation were based on 2D analysis using echocardiography and suggested a relation between LVT formation and abnormal flow profiles [6,8]. In the current study, we investigated 3D vortex ring formation quantitatively with 4D flow CMR. Our results demonstrated that the vortex ring during E-wave was less tilted to the LV in MI-LVT(+) group compared to MI-LVT(-) group. This implies that MI-LVT(+) patients have less eccentric inflow through the mitral valve, which can have an impact on the intraventricular flow patterns, and in particular distribution of LV flow components. Thus, existence of LVT in MI patients may alter the efficiency of LV blood flow transport. These results need to be extended by future research.

Despite advances in coronary reperfusion strategies and the use of concomitant dual antiplatelet therapy, LVT continues to occur in a significant number of MI patients [27]. Notably, MI-LVT(+) is of a high-risk cohort, as LVT formation is associated with an increased risk of thromboembolism as well as adverse clinical events [2,28]. Using the 4D flow CMR technique, we were able to characterize intra-cardiac flow comprehensively and observed altered LV global flow parameters in MI-LVT(+) patients, which may prove to be useful subclinical markers of intraventricular thrombosis after MI. Future studies are needed to further characterize LV flow changes in this specific cohort and to assess whether these parameters can be translated into clinical management.

4.1. Limitations

This study included a relatively small sample size and lacked a sex-matched comparison between the groups. However, the study was designed as an explorative study to provide novel, mechanistic perspectives regarding 4D LV flow characterization in chronic MI patients with/without LVT. Another limitation is that the myocardial infarct

location was heterogeneous across the MI patients, yet all LVT formations were apical. The peak vorticity values are likely to be underestimated due to the limited temporal resolution of 4D-flow data acquisition. Finally, the acquisition and whole post-processing time of the 4D flow data were long (e.g., >20 min. and > 60 min, respectively).

5. Conclusion

Chronic MI patients with LVT manifest a different arrangement of LV flow components. Vorticity vector fields are significantly reduced in MI patients but reveal an augmented pattern in patients with thrombus. Additionally, diastolic vortex ring geometric properties are altered in MI patients with LVT. These 4D flow analysis parameters advance the understanding of the post-MI LVT formation and persistence. The clinical value of these parameters should be tested by future work.

Funding

This work was supported by the British Heart Foundation [FS/10/62/28409 to S.P.] and Dutch Technology Foundation (STW), project number 11626 (JW, ME).

CRediT authorship contribution statement

Ahmet Demirkiran: Conceptualization, Data curation, Writing – original draft, Visualization, Project administration, Writing – review & editing, Formal analysis. **Mariëlla E.C.J. Hassell:** Conceptualization, Data curation, Writing – original draft, Project administration, Writing – review & editing. **Pankaj Garg:** Conceptualization, Data curation, Visualization, Project administration, Writing – review & editing, Software. **Mohammed S.M. Elbaz:** Conceptualization, Visualization, Funding acquisition. **Ronak Delewi:** Writing – review & editing. **John P. Greenwood:** Writing – review & editing. **Jan J. Piek:** Writing – review & editing. **Sven Plein:** Funding acquisition, Writing – review & editing. **Rob J. van der Geest:** Conceptualization, Data curation, Project administration, Visualization, Writing – review & editing, Software. **Robin Nijveldt:** Conceptualization, Data curation, Project administration, Writing – review & editing, Supervision.

Appendix A. Supplementary material

Supplementary data to this article can be found online at https://doi.org/10.1016/j.ejrad.2022.110233.

References

[1] J.R. Stratton, A.D. Resnick, Increased embolic risk in patients with left ventricular thrombi, Circulation 75 (5) (1987) 1004–1011.
[2] Maniwa N, Fujino M, Nakai M, et al. Anticoagulation combined with antiplatelet therapy in patients with left ventricular thrombus after first acute myocardial infarction. Eur Heart J. 2018;39(3):201-8.
[3] H. Bulluck, M.H.H. Chan, V. Paradies, R.L. Yellon, H.H. Ho, M.Y. Chan, C.W. L. Chin, J.W. Tan, D.J. Hausenloy, Incidence and predictors of left ventricular thrombus by cardiovascular magnetic resonance in acute ST-segment elevation myocardial infarction treated by primary percutaneous coronary intervention: a meta-analysis, J. Cardiovasc. Magn. Reson. 20 (1) (2018), https://doi.org/10.1186/s12968-018-0494-3.
[4] Demirkiran A, Everaars H, Amier RP, et al. Cardiovascular magnetic resonance techniques for tissue characterization after acute myocardial injury. Eur Heart J Cardiovasc Imaging. 2019;20(7):723-34.
[5] Garg P, van der Geest RJ, Swoboda PP, et al. Left ventricular thrombus formation in myocardial infarction is associated with altered left ventricular blood flow energetics. Eur Heart J Cardiovasc Imaging. 2019;20(1):108-17.
[6] B.J. Delemarre, C.A. Visser, H. Bot, A.J. Dunning, Prediction of apical thrombus formation in acute myocardial infarction based on left ventricular spatial flow pattern, J. Am. Coll. Cardiol. 15 (2) (1990) 355–360.
[7] S.S. Maze, M.N. Kotler, W.R. Parry, Flow characteristics in the dilated left ventricle with thrombus: qualitative and quantitative Doppler analysis, J. Am. Coll. Cardiol. 13 (4) (1989) 873–881.
[8] J.M. Van Dantzig, B.J. Delemarre, H. Bot, R.W. Koster, C.A. Visser, Doppler left ventricular flow pattern versus conventional predictors of left ventricular thrombus after acute myocardial infarction, J. Am. Coll. Cardiol. 25 (6) (1995) 1341–1346.
[9] L.C. Amado, B.L. Gerber, S.N. Gupta, D.W. Rettmann, G. Szarf, R. Schock, K. Nasir, D.L. Kraitchman, J.A.C. Lima, Accurate and objective infarct sizing by contrast-enhanced magnetic resonance imaging in a canine myocardial infarction model, J. Am. Coll. Cardiol. 44 (12) (2004) 2383–2389.
[10] M.A. Bernstein, X.J. Zhou, J.A. Polzin, K.F. King, A. Ganin, N.J. Pelc, G.H. Glover, Concomitant gradient terms in phase contrast MR: analysis and correction, Magn. Reson. Med. 39 (2) (1998) 300–308.
[11] M. Markl, R. Bammer, M.T. Alley, C.J. Elkins, M.T. Draney, A. Barnett, M. E. Moseley, G.H. Glover, N.J. Pelc, Generalized reconstruction of phase contrast MRI: analysis and correction of the effect of gradient field distortions, Magn Reson Med. 50 (4) (2003) 791–801.
[12] J.M. Peeters, C. Bos, C.J.G. Bakker, Analysis and correction of gradient nonlinearity and B0 inhomogeneity related scaling errors in two-dimensional phase contrast flow measurements, Magn Reson Med. 53 (1) (2005) 126–133.
[13] J. Eriksson, C.J. Carlhäll, P. Dyverfeldt, J. Engvall, A.F. Bolger, T. Ebbers, Semi-automatic quantification of 4D left ventricular blood flow, J. Cardiovas. Magnetic Resonance 12 (1) (2010) 9.
[14] S. Klein, M. Staring, K. Murphy, M.A. Viergever, J. Pluim, elastix: a toolbox for intensity-based medical image registration, IEEE Trans. Med. Imag. 29 (1) (2010) 196–205.
[15] J. Eriksson, A.F. Bolger, T. Ebbers, C.J. Carlhall, Four-dimensional blood flow-specific markers of LV dysfunction in dilated cardiomyopathy, Eur. Heart J. Cardiovasc. Imag. 14 (5) (2013) 417–424.
[16] A. Demirkiran, R.P. Amier, M.B.M. Hofman, R.J. van der Geest, L.F.H.J. Robbers, L. H.G.A. Hopman, M.J. Mulder, P. van de Ven, C.P. Allaart, A.C. van Rossum, M.J. W. Götte, R. Nijveldt, Altered left atrial 4D flow characteristics in patients with paroxysmal atrial fibrillation in the absence of apparent remodeling, Sci. Rep. 11 (1) (2021), https://doi.org/10.1038/s41598-021-85176-8.
[17] M.S.M. Elbaz, R.J. van der Geest, E.E. Calkoen, A. de Roos, B.P.F. Lelieveldt, A.A. W. Roest, J.J.M. Westenberg, Assessment of viscous energy loss and the association with three-dimensional vortex ring formation in left ventricular inflow: In vivo evaluation using four-dimensional flow MRI, Magn. Reson. Med. 77 (2) (2017) 794–805.
[18] M.S.M. Elbaz, E.E. Calkoen, J.J.M. Westenberg, B.P.F. Lelieveldt, A.A.W. Roest, R. J. van der Geest, Vortex flow during early and late left ventricular filling in normal subjects: quantitative characterization using retrospectively-gated 4D flow cardiovascular magnetic resonance and three-dimensional vortex core analysis, J. Cardiovas. Magnetic Resonance 16 (1) (2014) 78.
[19] B.E. Fenster, J. Browning, J.D. Schroeder, M. Schafer, C.A. Podgorski, J. Smyser, L. J. Silveira, J.K. Buckner, J.R. Hertzberg, Vorticity is a marker of right ventricular diastolic dysfunction, American J. Physiol.-Heart Circulatory Physiol. 309 (6) (2015) H1087–H1093.
[20] Schäfer M, Humphries S, Stenmark KR, et al. 4D-flow cardiac magnetic resonance-derived vorticity is sensitive marker of left ventricular diastolic dysfunction in patients with mild-to-moderate chronic obstructive pulmonary disease. European Heart Journal - Cardiovascular Imaging. 2017;19(4):415-24.
[21] R. Delewi, R. Nijveldt, A. Hirsch, C.B. Marcu, L. Robbers, M.E.C.J. Hassell, R.H. A. de Bruin, J. Vleugels, A.M. van der Laan, B.J. Bouma, R.A. Tio, J.G.P. Tijssen, A. C. van Rossum, F. Zijlstra, J.J. Piek, Left ventricular thrombus formation after acute myocardial infarction as assessed by cardiovascular magnetic resonance imaging, Eur. J. Radiol. 81 (12) (2012) 3900–3904.
[22] A. Bolger, E. Heiberg, M. Karlsson, L. Wigström, J. Engvall, A. Sigfridsson, T. Ebbers, J.-P. Kvitting, C.J. Carlhäll, B. Wranne, Transit of blood flow through the human left ventricle mapped by cardiovascular magnetic resonance, J. Cardiovasc. Magn. Reson. 9 (5) (2007) 741–747.
[23] V.M. Stoll, A.T. Hess, C.T. Rodgers, M.M. Bissell, P. Dyverfeldt, T. Ebbers, S. G. Myerson, C.-J. Carlhäll, S. Neubauer, Left Ventricular Flow Analysis, Circ Cardiovasc Imaging. 12 (5) (2019), https://doi.org/10.1161/CIRCIMAGING.118.008130.
[24] E. Svalbring, A. Fredriksson, J. Eriksson, P. Dyverfeldt, T. Ebbers, A.F. Bolger, J. Engvall, C.-J. Carlhäll, A. Aliseda, Altered Diastolic Flow Patterns and Kinetic Energy in Subtle Left Ventricular Remodeling and Dysfunction Detected by 4D Flow MRI, PLoS ONE 11 (8) (2016) e0161391.
[25] P. Garg, S. Crandon, P.P. Swoboda, G.J. Fent, J.R.J. Foley, P.G. Chew, L.A. E. Brown, S. Vijayan, M.E.C.J. Hassell, R. Nijveldt, M. Bissell, M.S.M. Elbaz, A. Al-Mohammad, J.J.M. Westenberg, J.P. Greenwood, R.J. van der Geest, S. Plein, E. Dall'Armellina, Left ventricular blood flow kinetic energy after myocardial infarction - insights from 4D flow cardiovascular magnetic resonance, J. Cardiovasc. Magn. Reson. 20 (1) (2018), https://doi.org/10.1186/s12968-018-0483-6.
[26] V.P. Kamphuis, M.S.M. Elbaz, P.J. van den Boogaard, L.J.M. Kroft, H.J. Lamb, M. G. Hazekamp, M.R.M. Jongbloed, N.A. Blom, W.A. Helbing, A.A.W. Roest, J.J. M. Westenberg, Stress increases intracardiac 4D flow cardiovascular magnetic resonance -derived energetics and vorticity and relates to VO2max in Fontan patients, J. Cardiovasc. Magn. Reson. 21 (1) (2019), https://doi.org/10.1186/s12968-019-0553-4.
[27] C.P. McCarthy, M. Vaduganathan, K.J. McCarthy, J.L. Januzzi Jr., D.L. Bhatt, J. W. McEvoy, Left Ventricular Thrombus After Acute Myocardial Infarction: Screening, Prevention, and Treatment, JAMA Cardiol. 3 (7) (2018) 642–649.
[28] J. Poss, S. Desch, C. Eitel, S. de Waha, H. Thiele, I. Eitel, Left Ventricular Thrombus Formation After ST-Segment-Elevation Myocardial Infarction: Insights From a Cardiac Magnetic Resonance Multicenter Study, Circ Cardiovasc Imaging. 8 (10) (2015), e003417.